Two-Dimensional Detailed Numerical Simulation on Ammonia/Hydrogen/Air Detonation

Go. Inoue[1], Nobuyuki. Tsuboi[1], Kohei. Ozawa[1], A. Koichi. Hayashi[2]
[1] Kyushu Institute of Technology, 1-1, Sensui-cho,Tobata-ku, Kitakyushu-shi, Fukuoka, 804-8550, Japan
[2] Aoyama Gakuin University, 4-4-25 Shibuya, Shibuya-ku, Tokyo, 150-8366, Japan

1 Introduction

Detonation is a type of premixed combustion and is characterized by high temperature and high pressure compared to deflagration. If detonation occurs unintentionally, it may lead to a major accident due to the above characteristics. In fact, in 2001, an explosion accident was reported at Hamaoka Nuclear Power Plant Unit 1[1] that was thought to be caused by a detonation. Therefore, understanding detonation characteristics are very important from the viewpoint of safety engineering.

The purpose of this study is to understand the detonation characteristics to use ammonia as a fuel. Ammonia is a carbon-free fuel that does not emit carbon dioxide when ammonia is burned. Ammonia is expected to be a next-generation fuel because ammonia can be transported and stored easily and its industrial manufacturing methods have already been established. However, ammonia has the disadvantage that ammonia is a toxic gas and it is relatively difficult to burn. The present study is to calculate the two-dimensional detonation for ammonia/hydrogen/air mixture to understand the feature of ammonia oxidation in a high-pressure situation.

2 Numerical Method

The present governing equations are the two-dimensional compressible Euler equations with species conservation equations. The numerical flux for the convective term uses the hybrid method combining the Harten-Lax-van-Leer-contact (HLLC) [2] and the local Lax-Friedrich (LLF) scheme. Its accuracy is increased by the fifth-order weighted compact nonlinear scheme (WCNS) [3-10]. The fourth-order TVD Runge-Kutta method [11] is used for the time integration method to increase numerical robustness. The chemical reaction source term is integrated by the Extended Robustness-Enhanced Numerical Algorithm (ERENA) [12]. The chemical reaction model adopts the UT-LCS model [13], which can predict the laminar flame speeds and the ignition delay times of ammonia/hydrogen/air combustion under the high-pressure. The model has 32 species and 213 elementary reactions. The Cantera library[14] is used to solve this chemical reaction because the Cantera supports the PLOG function in this reaction model.

Figure 1 shows the calculation domain of this study. In this study, the shock wave coordinate system is used to reduce the calculation cost. The boundary conditions of the top and bottom walls use slip and

Correspondence to: inoue.go558@mail.kyutech.jp

adiabatic wall conditions. Outlet condition at the left-side boundary is decided by referring to the conditions of Gamezo et al [14]. Y_b, Y_1, and Y_e mean every boundary value, the current in the first cell near the boundary, and the extrapolation limit, respectively. The unburned gas is composed of NH_3/H_2/air premixed gas which is 1 atm and 300 K. A small source of unburned gas is placed behind the shock wave to create a small disturbance to start the detonation. The unburned gas enters with Chapman-Jouguet (C-J) detonation velocity from the inlet side at the right boundary. The one-dimensional numerical results are also used to start the two-dimensional detonation.

Table 1 shows the calculation cases of this study. From cases #1 to #6, the detonation does not appear in the one-dimensional calculation. So we mainly discuss the result between cases #7 and #10. The grid width for each case is determined to include 100 grid points in the induction distance. The channel width uses 0.36 times the detonation cell size because a past study [16] shows that the channel width at the detonation propagation limit is about 1/3 of the cell size. The detonation cell size is estimated from the experimental value [17] and its induction distance as shown in Fig. 2.

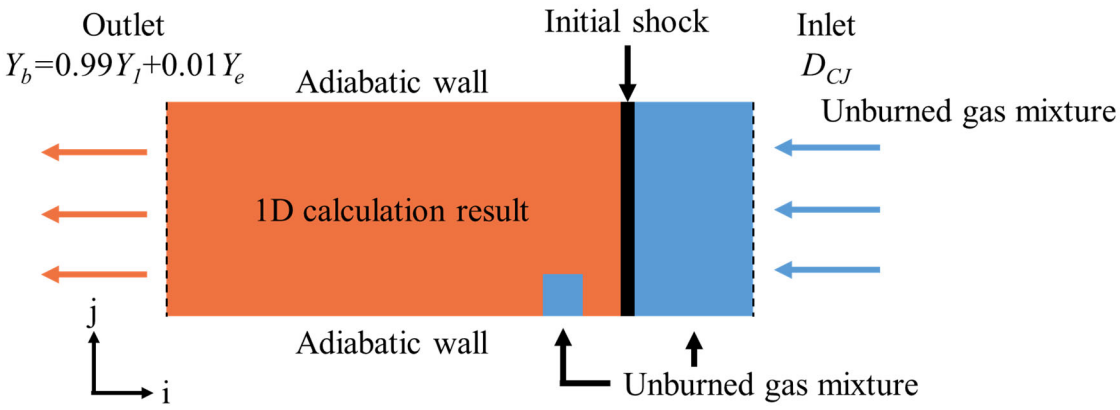

Figure 1: Present calculation area and boundary conditions.

Table 1: Simulation conditions. α is expressed by the following equation:

$$4\left((1-\alpha)\mathrm{NH_3}+\alpha\mathrm{H_2}\right)+3(\mathrm{O_2}+3.76\mathrm{N_2})$$

Case	α	Induction distance [m]	1-D detonation	Grid width [μm]	Grid points (imax x jmax)
#1	0	0.0695	No	-	-
#2	0.1	0.0163	No	-	-
#3	0.2	0.00876	No	-	-
#4	0.3	0.00556	No	-	-
#5	0.4	0.00380	No	-	-
#6	0.5	0.00261	No	-	-
#7	0.6	0.00181	Go	18.0	1666 x 333
#8	0.7	0.00122	Go	12.1	1666 x 333
#9	0.8	0.000822	Go	8.2	1666 x 333
#10	0.9	0.000603	Go	6.0	1666 x 333

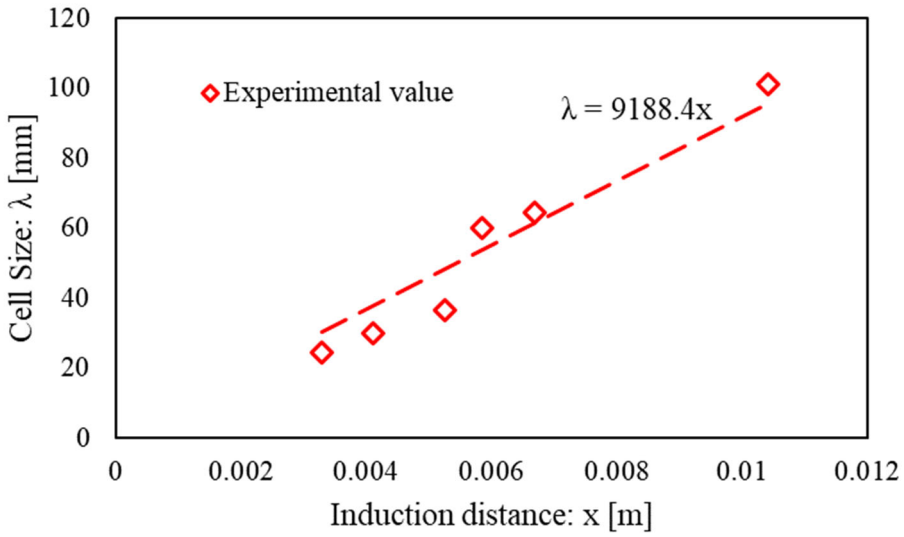

Figure 2: Estimate detonation cell size from experimental value [14] and induction distance.

3 Results and Discussion

3.1 Temperature distribution of chemical species

In order to understand the characteristics of chemical species in the NH_3/H_2/air detonation, the mass fractions of some important chemical species are plotted as a function of temperature.

Figure 3 shows the instantaneous NH_3 mass fraction as a function of temperature for each case. From Fig. 3, it can be seen that the decomposition of NH_3 starts at approximately 1300 K and is mostly consumed at the temperature of 2500-3000 K. Comparing cases #7 and #10, it can be seen that the mass fraction of NH_3 in the high-temperature region is small in case #10. So, from this, it can be seen that the decomposition reaction of NH_3 is promoted by H_2.

Figure 4 shows the instantaneous NH_2 mass fraction as a function of temperature for each case. NH_2 plays a key role to reduce the concentration of NO [13]. In Fig. 4, it can be observed that NH_2 generates at approximately 1500 K and consumes at 2500-3000 K. Comparing cases #7 and #10, it can be seen that the maximum NH_2 for case #10 is smaller than that for case #7. From this, it is considered that the addition of H_2 promotes the reaction of not only NH_3 but also intermediate products such as NH_2.

Figure 5 shows the instantaneous NO mass fraction as a function of temperature for each case. In Fig. 5, the difference between cases #7 and #10 is small, however, the amount of NO mass fraction increases with increasing the temperature.

3.2 Maximum pressure history

Figure 6 shows the maximum pressure histories for cases #8 and case #9. Comparing these two cases, it can be seen that the cell shape is irregular for case #8. The cell shape is generally more irregular as the activation energy increases. So, it is thought that increasing the mixing ratio of H_2 leads to a decrease in the activation energy of the premixed gas, however, the activation energy will be calculated by the ZND in the future.

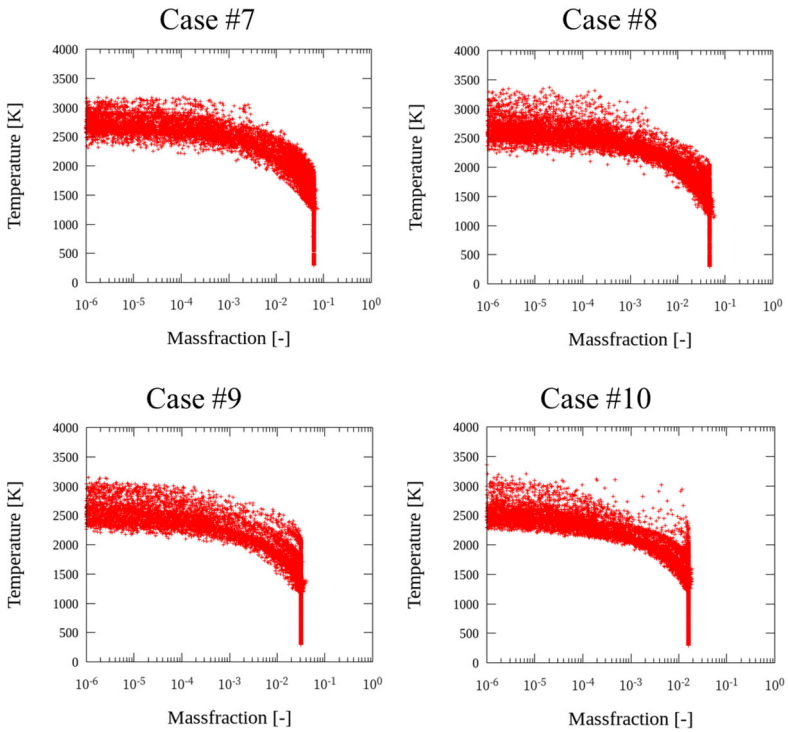

Figure 3: NH_3 mass fraction distributions as a function of temperature.

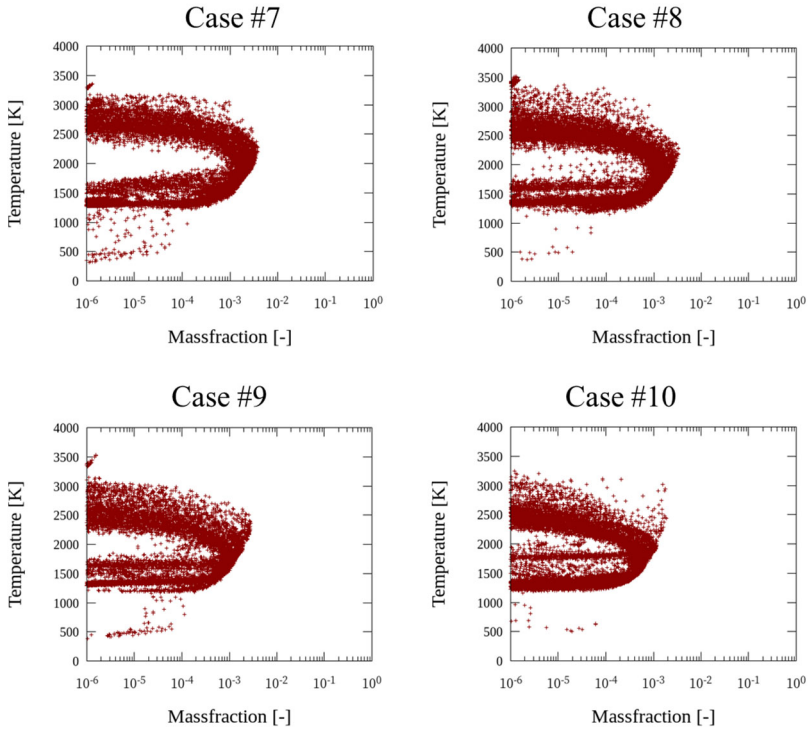

Figure 4: NH_2 mass fraction distributions as a function of temperature.

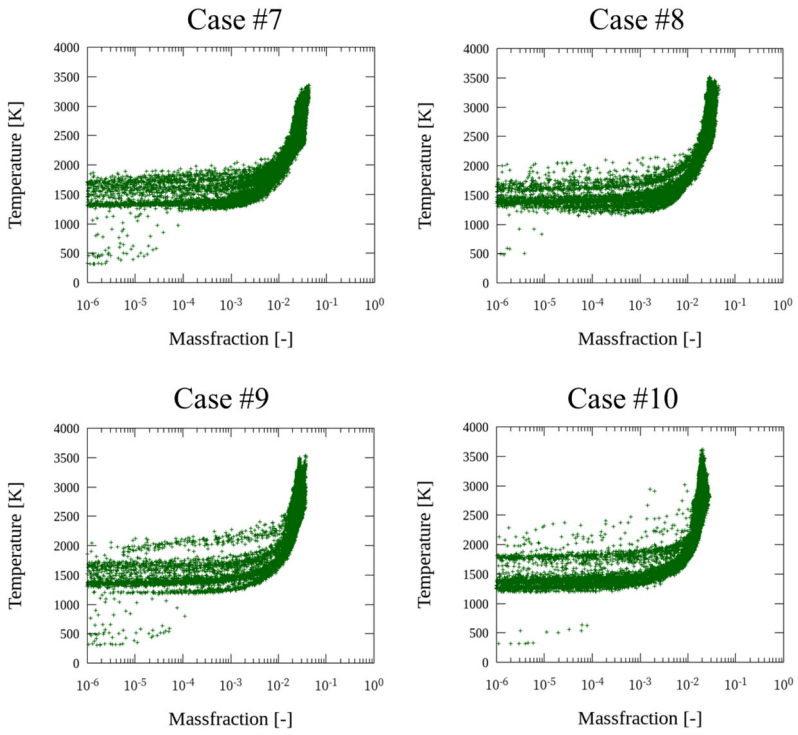

Figure 5: NO mass fraction distributions as a function of temperature.

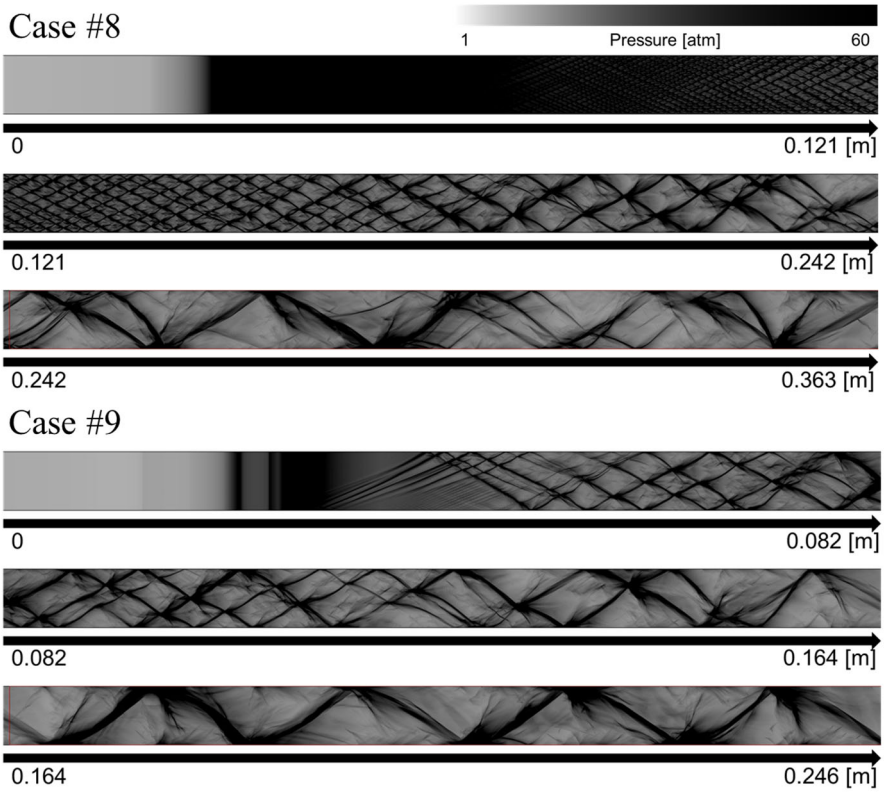

Figure 6: Maximum pressure histories of cases #8 and #9.

4 Conclusions

Two-dimensional detailed numerical simulations of NH_3/H_2/air detonation are performed and the results are summarized as follows:

(1) Increasing the mixing ratio of H_2 promotes the decomposition reaction of NH_3.

(2) Increasing the H_2 mixing ratio increases the amount of produced NH_2, and as a result, the amount of NO production is decreased.

(3) Increasing the H_2 concentration leads the regular cellular structure in the detonation.

Acknowledgments

This study was carried out using the Oakbridge-CX system, which is a large-scale computing system of the University of Tokyo.

References

[1] Report of Examination of the Ruptured Pipe at the Hamaoka Nuclear Power Station Unit-1, JAERI-Tech 2001-094, 2001.

[2] E.F. Toro, M. Spruce, W. Speares (1994). Shock Waves 4: 25-34.

[3] X. Deng, H. Zhang (2000). Journal of Computational Physics165: 22–44.

[4] S. Zhang, S. Jiang, C-W. Shu (2008). Journal of Computational Physics 227: 7294-7321.

[5] T. Nonomura, K. Fujii (2013). Computers & Fluids 85: 8-18.

[6] T. Nonomura, K. Fujii (2009). Journal of Computational Physics 228: 3533-3539.

[7] T. Nonomura, N. Iizuka, K. Fujii (2010). Computers & Fluids 39: 197–21.

[8] T. Niibo, Y. Morii, M. Asahara, N. Tsuboi, A. K. Hayashi (2016). Combustion Science and Technology 188: 2044-2059.

[9] R. Iida, M. Asahara, A. K. Hayashi, N. Tsuboi (2014). Combustion Science and Technology 186: 1736-1757.

[10] N. Takeshima, K. Ozawa, N. Tsuboi, A.K. Hayashi, Y. Morii(2020). Shock Waves 30: 809-824.

[11] S. Gottlieb, D. I. Ketcheson, C-W. Shu (2009). Journal of Scientific Computing volume 38: 251–289.

[12] Y. Morii, H. Terashima, M. Koshi, T. Shimizu, E. Shima(2016). Journal of Computational Physics 322: 547-558.

[13] J. Otomo, M. Koshi, T. Mitsumori, H. Iwasaki, K. Yamada (2018). International Journal of Hydrogen Energy 43: 3004-3014.

[14] D. G. Goodwin, R. L. Speth, H. K. Moffat, B. W. Weber(2021), https://www.cantera.org, version 2.5.1.

[15] V. Gamezo, D. Desbordes, E. Oran (1999). Combution and Flame 116: 154-165.

[16] Y. Gao, H. D. Ng, J. H. S. Lee (2014). Shock Waves 24: 447-454.

[17] R. Akbar, M. Kaneshige, E. Schultz, J. Shepherd (1997). Explosion Dynamics Laboratory Report FM97-3.